

Supporting Information for

**A new perspective for evaluating photoelectric performance of
organic-inorganic hybrid perovskites based on DFT calculations of
excited states**

Zhengyang Gao^a, Shengyi Chen^a, Yang Bai^a, Min Wang^a, Xiaoshuo Liu^{a,b}, Weijie Yang^{*a}, Wei Li^c, Xunlei Ding^{*c},
Jianxi Yao^{*d,e}

a Department of Power Engineering, School of Energy, Power and Mechanical Engineering, North China Electric Power University, Baoding 071003, China

b Key Laboratory of Energy Thermal Conversion and Control of Ministry of Education, School of Energy and Environment, Southeast University, Nanjing 210096, China

c Institute of Clusters and Low Dimensional Nanomaterials, School of Mathematics and Physics, North China Electric Power University, Beijing, People's Republic of China

d State Key Laboratory of Alternate Electrical Power System with Renewable Energy Sources, North China Electric Power University, Beijing 102206, China.

e Beijing Key Laboratory of Energy Safety and Clean Utilization, North China Electric Power University, Beijing 102206, China.

Table S3 The binding energy table which is calculated by the formula $\Delta E = E_{ABX_3} - E_A - E_{BX_3}$. M06-2X-D3, M06-2X, B3LYP-D3, and B3LYP are the testing functionals. Error is the difference between the binding energy calculated by other functionals and M06-2X-D3. (all energies are in eV) Time is job cpu time which is exported by Gaussian 09.

Cluster	M06-2X-D3			M06-2X		
	Binding energy	Error	Time (hours)	Binding energy	Error	Time (hours)
MAPbF ₃	5.886	0.000	0.640	5.881	0.005	0.628
MAPbCl ₃	4.989	0.000	0.602	4.982	0.007	0.559
MAPbBr ₃	4.770	0.000	0.871	4.763	0.007	0.992
MAPbI ₃	4.524	0.000	1.003	4.518	0.007	1.064
Cluster	B3LYP-D3			B3LYP		
	Binding energy	Error	Time (hours)	Binding energy	Error	Time (hours)
MAPbF ₃	5.866	0.020	0.444	5.684	0.201	0.402
MAPbCl ₃	5.100	0.112	0.381	4.819	0.169	0.373
MAPbBr ₃	4.888	0.118	0.710	4.579	0.191	0.606
MAPbI ₃	4.673	0.149	0.732	4.327	0.198	0.792

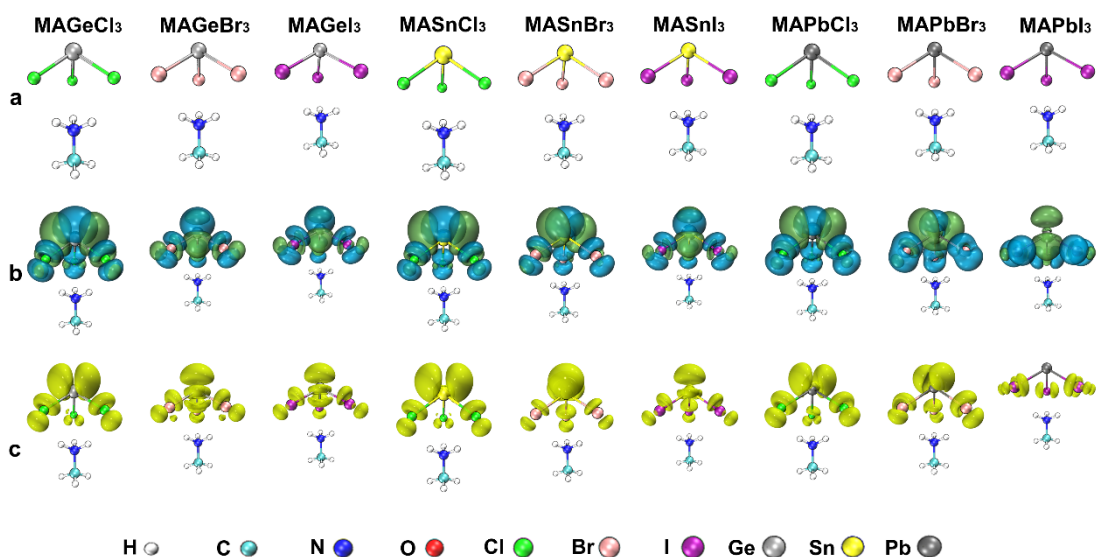


Figure S1. a) Optimized structures of MABX_3 ($\text{B} = \text{Ge}^{2+}, \text{Sn}^{2+}, \text{Pb}^{2+}$, and $\text{X} = \text{Cl}^-, \text{Br}^-, \text{I}^-$). b) The electron-hole distribution chart. Green and blue isosurfaces represent the distribution of electrons and holes, respectively. c) The $s(r)$ distribution charts. The yellow isosurface represents the overlap of electrons and holes. The isosurfaces were uniformly selected as 0.002, respectively.

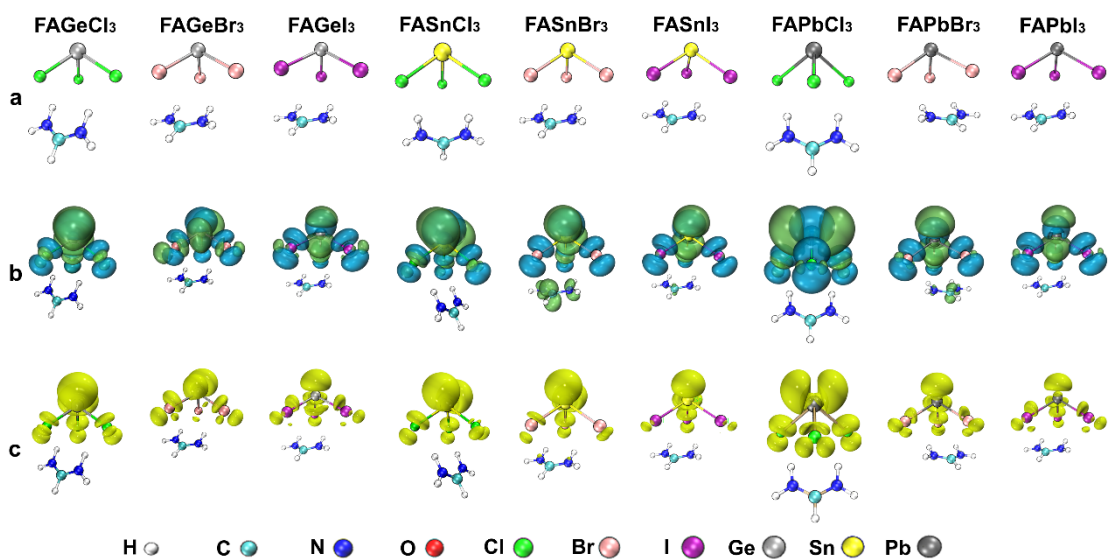


Figure S2. a) Optimized structures of FABX₃ (B = Ge²⁺, Sn²⁺, Pb²⁺, and X = Cl⁻, Br⁻, I⁻). b) The electron-hole distribution chart. Green and blue isosurfaces represent the distribution of electrons and holes, respectively. c) The $s(r)$ distribution charts. The yellow isosurface represents the overlap of electrons and holes. The isosurfaces were uniformly selected as 0.002, respectively.

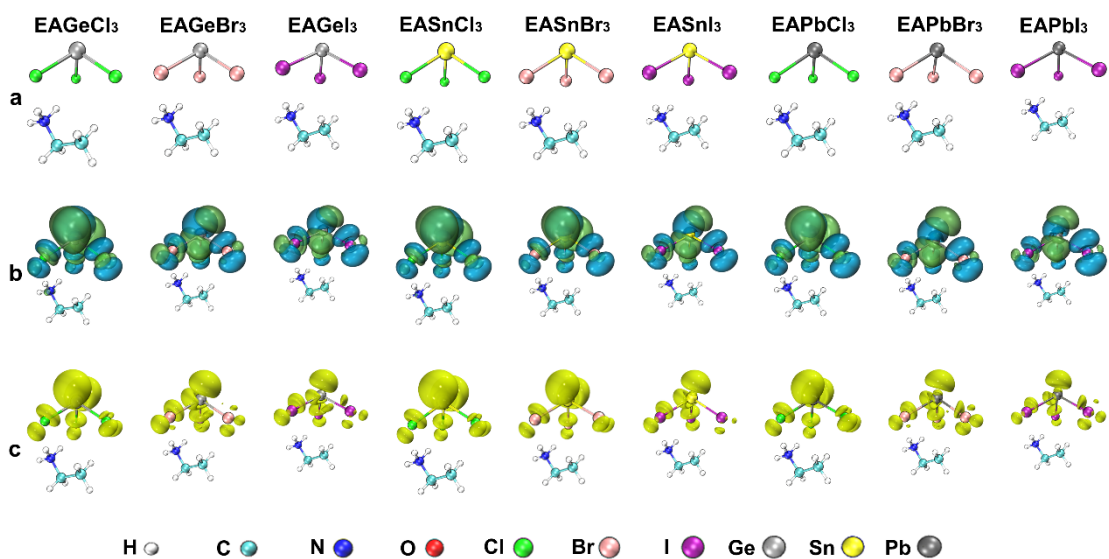


Figure S3. a) Optimized structures of EABX₃ (B = Ge²⁺, Sn²⁺, Pb²⁺, and X = Cl⁻, Br⁻, I⁻). b) The electron-hole distribution chart. Green and blue isosurfaces represent the distribution of electrons and holes, respectively. c) The $s(r)$ distribution charts. The yellow isosurface represents the overlap of electrons and holes. The isosurfaces were uniformly selected as 0.002, respectively.

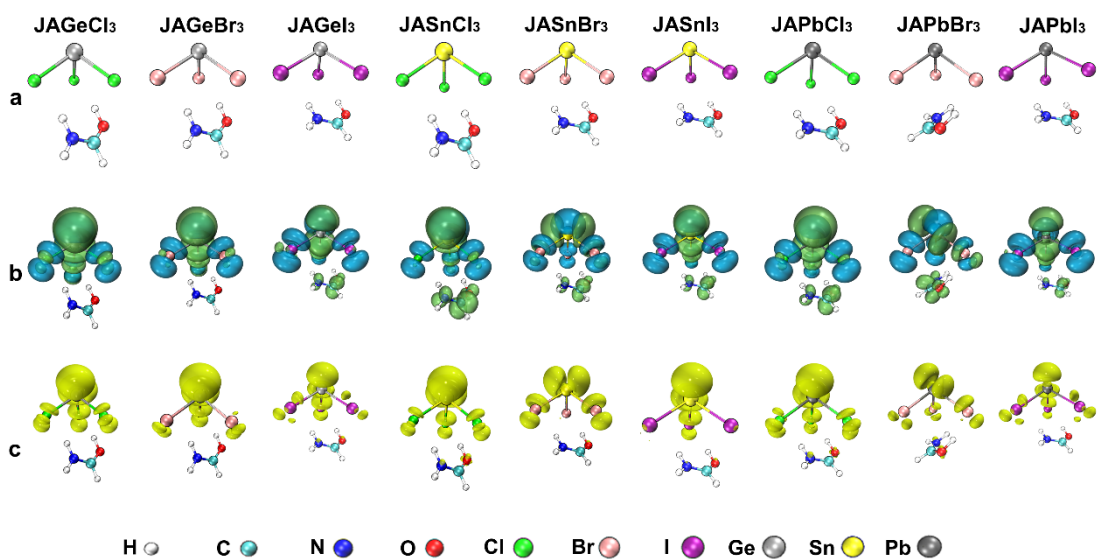


Figure S4. a) Optimized structures of JABX₃ (B = Ge²⁺, Sn²⁺, Pb²⁺, and X = Cl⁻, Br⁻, I⁻). b) The electron-hole distribution chart. Green and blue isosurfaces represent the distribution of electrons and holes, respectively. c) The $s(r)$ distribution charts. The yellow isosurface represents the overlap of electrons and holes. The isosurfaces were uniformly selected as 0.002, respectively.

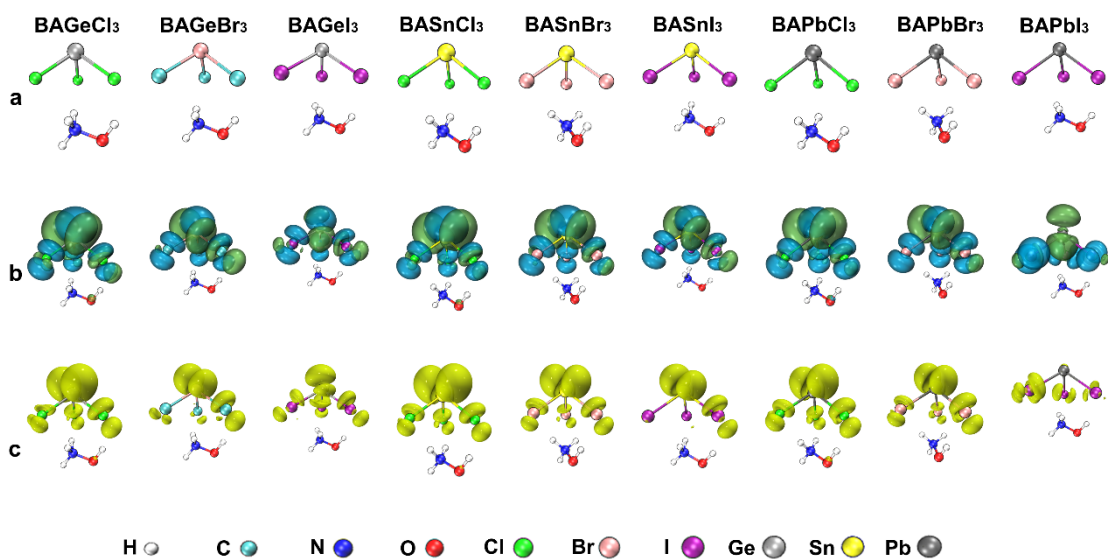


Figure S5. a) Optimized structures of BABX_3 ($\text{B} = \text{Ge}^{2+}, \text{Sn}^{2+}, \text{Pb}^{2+}$, and $\text{X} = \text{Cl}^-, \text{Br}^-, \text{I}^-$). b) The electron-hole distribution chart. Green and blue isosurfaces represent the distribution of electrons and holes, respectively. c) The $s(r)$ distribution charts. The yellow isosurfaces represent the overlap of electrons and holes. The isosurfaces were uniformly selected as 0.002, respectively.

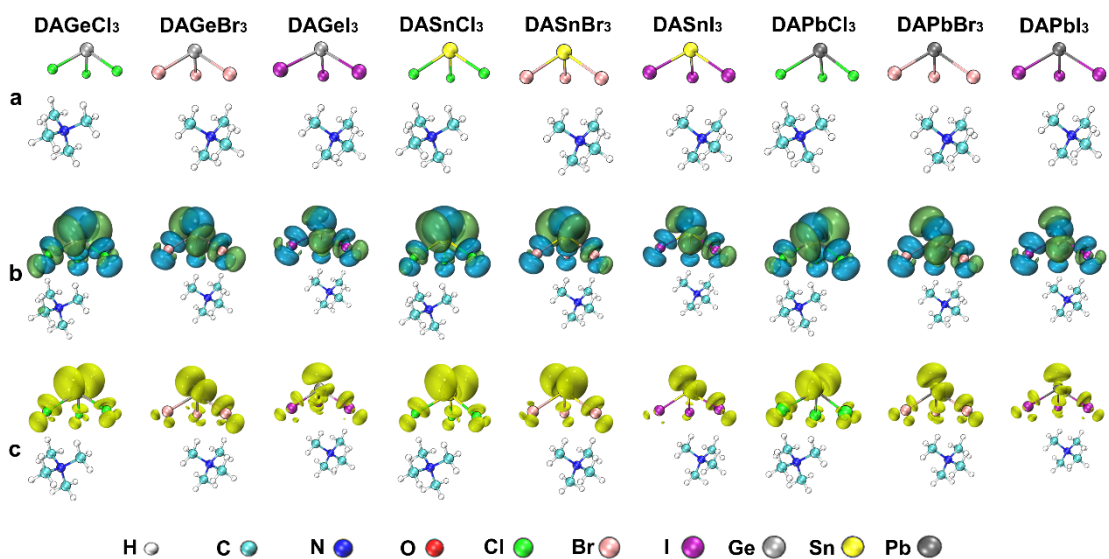


Figure S6. a) Optimized structures of DABX₃ (B = Ge²⁺, Sn²⁺, Pb²⁺, and X = Cl⁻, Br⁻, I⁻). b) The electron-hole distribution chart. Green and blue isosurfaces represent the distribution of electrons and holes, respectively. c) The $s(r)$ distribution charts. The yellow isosurface represents the overlap of electrons and holes. The isosurfaces were uniformly selected as 0.002, respectively.

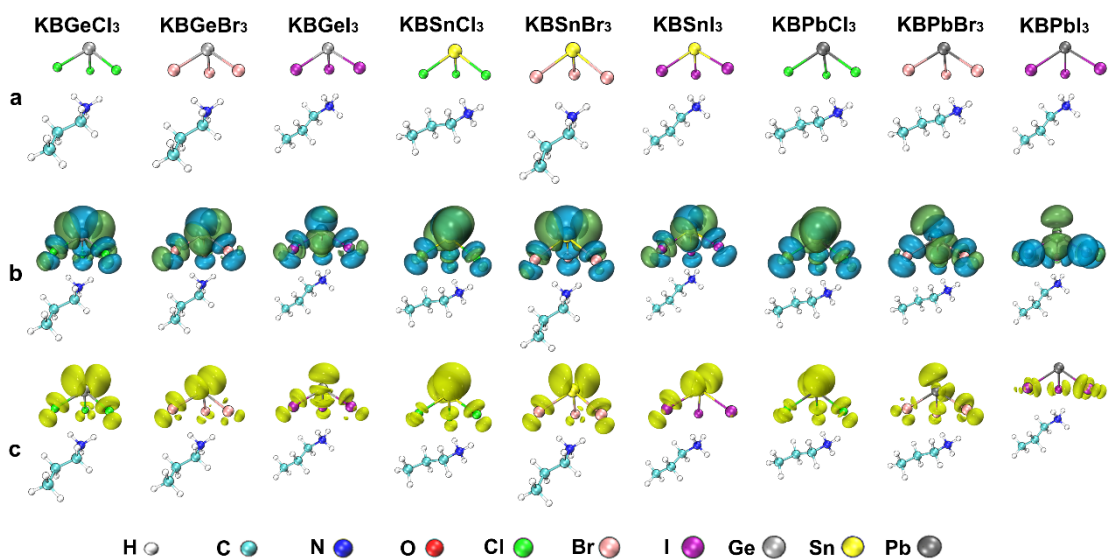


Figure S7. a) Optimized structures of KBBX₃ (B = Ge²⁺, Sn²⁺, Pb²⁺, and X = Cl⁻, Br⁻, I⁻). b) The electron-hole distribution chart. Green and blue isosurfaces represent the distribution of electrons and holes, respectively. c) The $s(r)$ distribution charts. The yellow isosurface represents the overlap of electrons and holes. The isosurfaces were uniformly selected as 0.002, respectively.

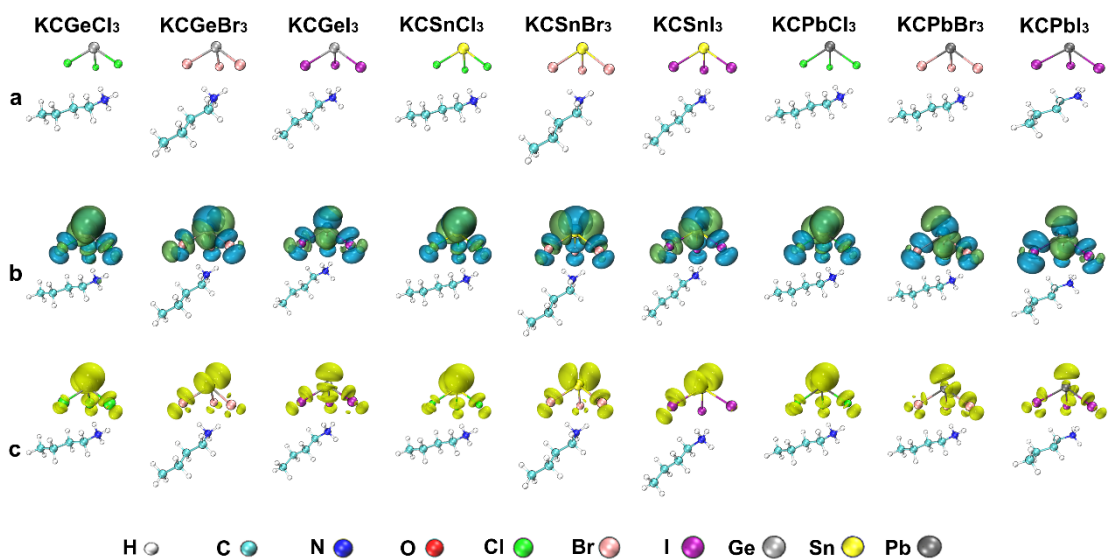


Figure S8. a) Optimized structures of KCBX₃ (B = Ge²⁺, Sn²⁺, Pb²⁺, and X = Cl⁻, Br⁻, I⁻). b) The electron-hole distribution chart. Green and blue isosurfaces represent the distribution of electrons and holes, respectively. c) The $s(r)$ distribution charts. The yellow isosurface represents the overlap of electrons and holes. The isosurfaces were uniformly selected as 0.002, respectively.

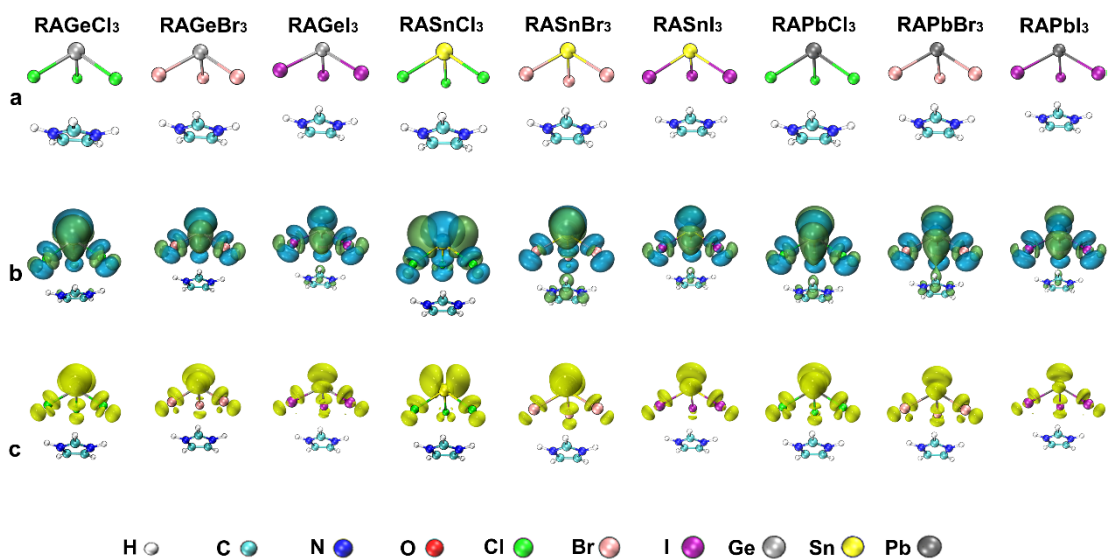


Figure S9. a) Optimized structures of RABX₃ (B = Ge²⁺, Sn²⁺, Pb²⁺, and X = Cl⁻, Br⁻, I⁻). b) The electron-hole distribution chart. Green and blue isosurfaces represent the distribution of electrons and holes, respectively. c) The $s(r)$ distribution charts. The yellow isosurface represents the overlap of electrons and holes. The isosurfaces were uniformly selected as 0.002, respectively.

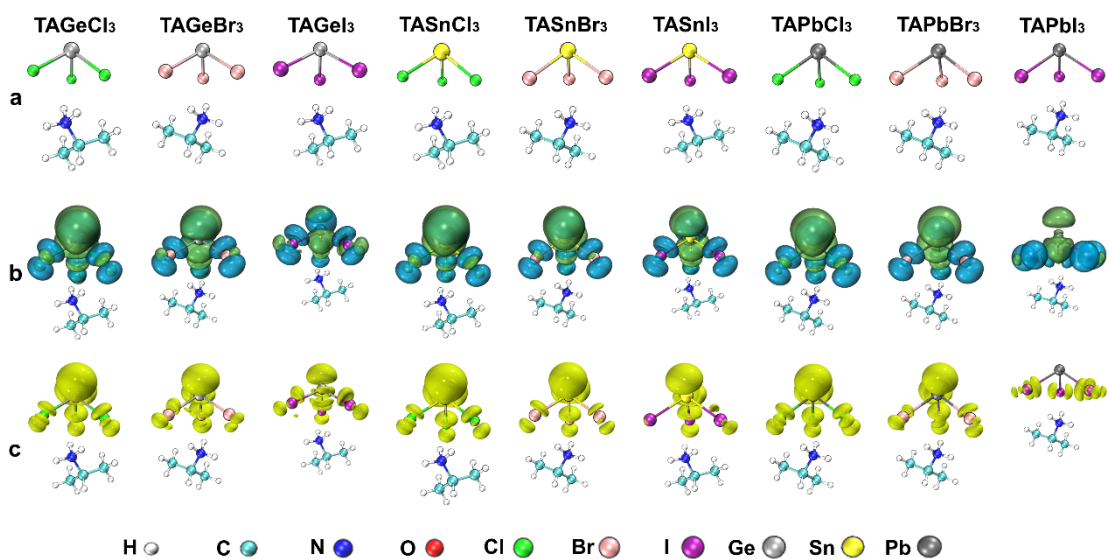


Figure S10. a) Optimized structures of TABX₃ (B = Ge²⁺, Sn²⁺, Pb²⁺, and X = Cl⁻, Br⁻, I⁻). b) The electron-hole distribution chart. Green and blue isosurfaces represent the distribution of electrons and holes, respectively. c) The $s(r)$ distribution charts. The yellow isosurface represents the overlap of electrons and holes. The isosurfaces were uniformly selected as 0.002, respectively.

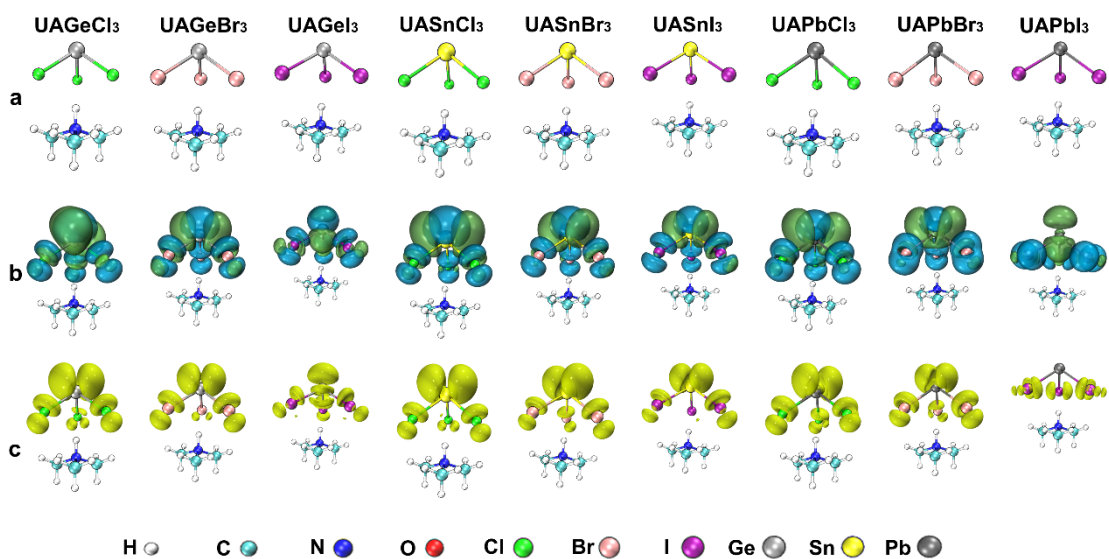
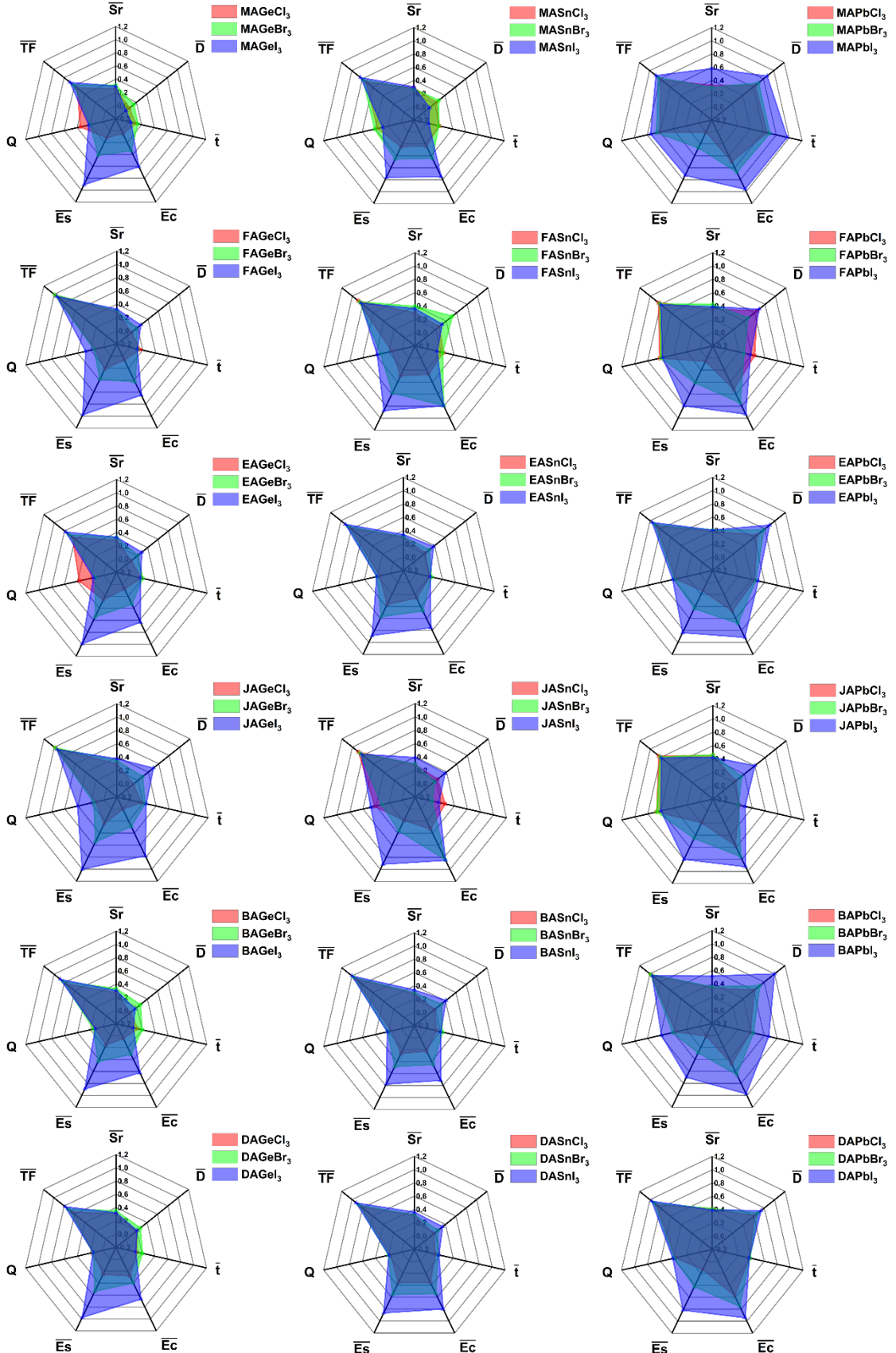


Figure S11. a) Optimized structures of UABX_3 ($\text{B} = \text{Ge}^{2+}, \text{Sn}^{2+}, \text{Pb}^{2+}$, and $\text{X} = \text{Cl}^-, \text{Br}^-, \text{I}^-$). b) The electron-hole distribution chart. Green and blue isosurfaces represent the distribution of electrons and holes, respectively. c) The $s(r)$ distribution charts. The yellow isosurface represents the overlap of electrons and holes. The isosurfaces were uniformly selected as 0.002, respectively.



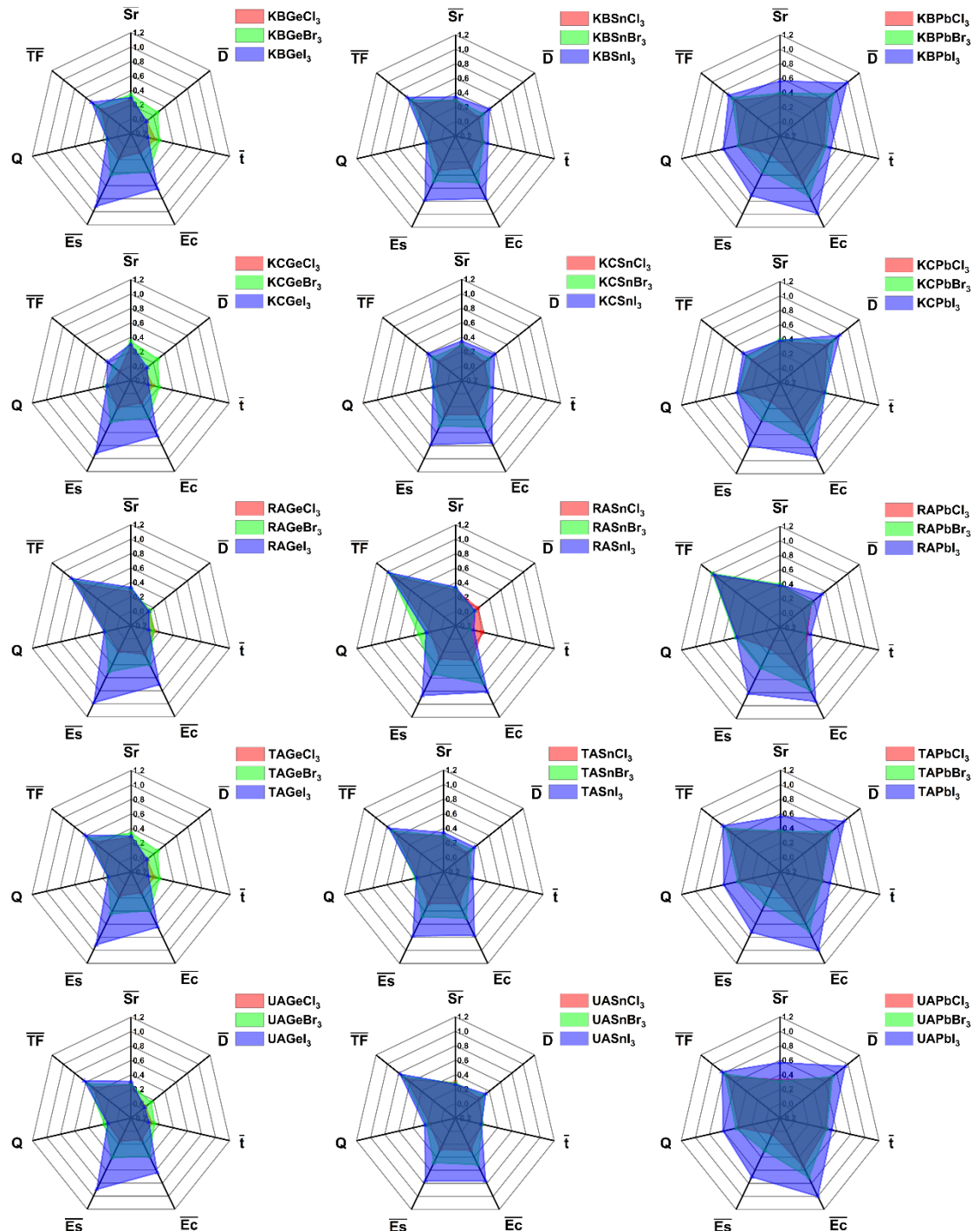


Figure S12. Radar chart of the normalized electronic excitation characteristic index. \bar{D} index means the centroid distance between holes and electrons. \bar{Sr} index means the separation between holes and electrons. \bar{TF} means the normalized tolerance factor. The Q index represents the net charge transfer. \bar{Ec} and \bar{Es} respectively represent the relative magnitude of exciton binding energy and excitation energy. \bar{t} index measures the degree of separation of holes and electrons.

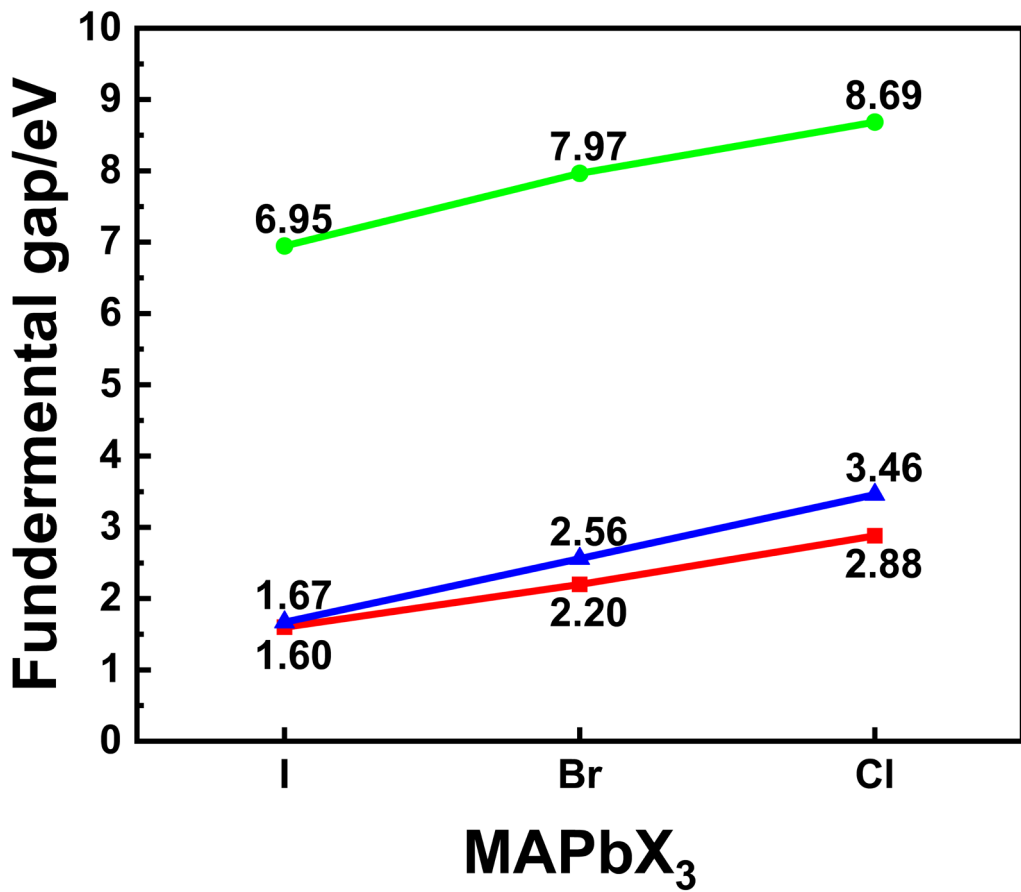


Figure S13. The DFT-M06-2X calculated HOMO-LUMO gaps (green) of the molecules compared to band gaps (blue) calculated by the DFT-GGA-GW with SOC and the experimental values (red).

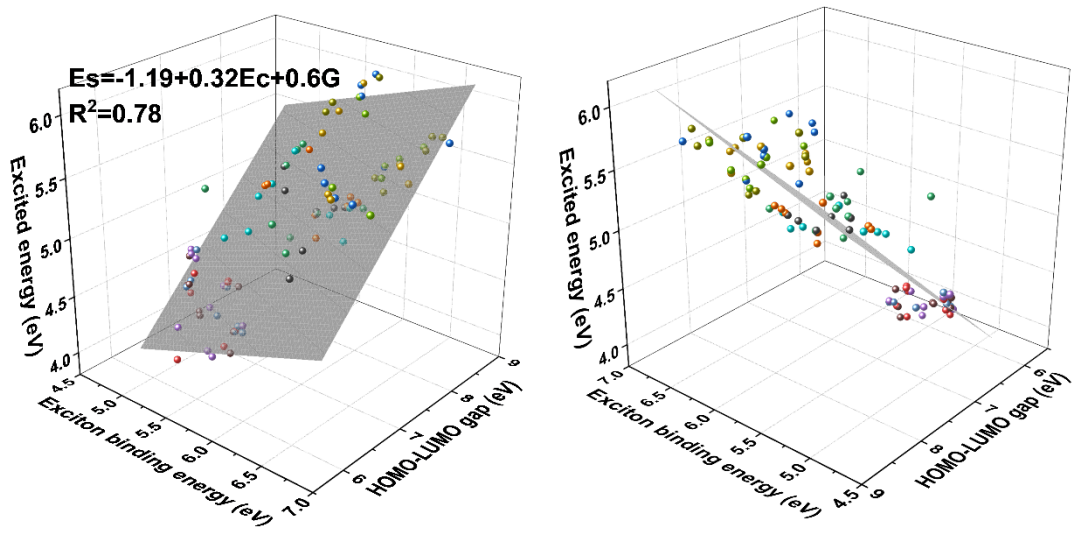


Figure S14 Two-dimensional plane fitting diagram between exciton binding energy, HOMO-LUMO gap, and excitation energy. E_s means the excited energy. E_c means the exciton binding energy and G represents the HOMO-LUMO gap.

Notes and references

1. A. M. Glazer, *Acta Crystallogr. Sect. B*, 1972, **28**, 3384–3392.
2. Markus B., Thorsten K., Michael W., *Dalton Trans.*, 2017, **46**, 3500-3509.
3. Shannon R D., *Acta Crystallogr. Sect. A*, 1976, **32**, 751-767.
4. A. Amat, E. Mosconi, E. Ronca, C. Quarti, P. Umari, Md. K. Nazeeruddin, M. Grätzel, F. De Angelis, *Nano lett.*, 2014, **14**, 3608-3616.
5. T. J. Jacobsson, M. Pazoki, A. Hagfeldt, T. Edvinsson, *J. Phys. Chem. C*, 2015, **119**, 25673-25683.
6. I. E. Collings, J. A. Hill, A. B.Cairns, R. I. Cooper, A. L. Thompson, J. E. Parker, C. C. Tang, A. L. Goodwin, *Dalton Trans.*, 2016, **45**, 4169-4178.